DOI: 10.1002/ange.201209846

VIP Methane Oxidation

Efficient Oxidation of Methane to Methanol by Dioxygen Mediated by Tricopper Clusters**

Sunney I. Chan, Yu-Jhang Lu, Penumaka Nagababu, Suman Maji, Mu-Cheng Hung, Marianne M. Lee, I-Jui Hsu, Pham Dinh Minh, Jeff C.-H. Lai, Kok Yoah Ng, Sridevi Ramalingam, Steve S.-F. Yu,* and Michael K. Chan**

Methane oxidation is extremely difficult chemistry to perform in the laboratory. The C–H bond in CH_4 has the highest bond energy (104 kcal mol^{-1}) amongst organic substrates. In nature, the controlled oxidation of organic substrates is mediated by an important class of enzymes known as monooxygenases and dioxygenases,[1] and the methane monooxygenases are unique in their capability to mediate the facile conversion of methane to methanol.[2,3] With a turnover frequency approaching 1 s^{-1}, the particulate methane monooxygenase (pMMO) is the most efficient methane oxidizer discovered to date. Given the current interest in developing a laboratory catalyst suitable for the conversion of methane to methanol on an industrial scale, there is strong impetus to understand how pMMO works and to develop functional biomimetics of this enzyme. pMMO is a complex membrane protein consisting of three subunits (PmoA, PmoB, and PmoC) and many copper cofactors.[3] Inspired by the proposal that the catalytic site might be a tricopper cluster, we have recently developed a series of tricopper complexes that are capable of supporting facile catalytic oxidation of hydrocarbons.[4,5] We show herein that these model tricopper complexes can mediate efficient catalytic oxidation of methane to methanol as well.

The oxidation of CH_4 mediated by the tricopper complex $[Cu^{I}Cu^{I}Cu^{I}($**7-N-Etppz**$)]^{1+}$ in acetonitrile (ACN), where **7-N-Etppz** corresponds to the ligand 3,3′-(1,4-diazepane-1,4-diyl)bis[1-(4-ethylpiperazine-1-yl)propan-2-ol], is summarized in Figure 1A. A single turnover (turnover number; TON = 0.92) is obtained when this $Cu^{I}Cu^{I}Cu^{I}$ complex is activated by excess dioxygen in the presence of excess CH_4 (Figure 1B). The reaction is complete within ten minutes, clearly indicating that the oxidation is very rapid. In accordance with the single turnover, the kinetics of the overall process is pseudo first-order with respect to the concentration of the fully reduced tricopper complex with a rate constant $k_1 = 0.065\ \text{min}^{-1}$ (Figure 1B, inset). If we assume that the kinetics is limited by the dioxygen activation of the $Cu^{I}Cu^{I}Cu^{I}$ cluster with the subsequent O-atom transfer to the substrate molecule being rapid, then $k_1 = k_2 \cdot [O_2]_0$, and from the solubility of oxygen in ACN at 25 °C (8.1 mM),[6] we obtain the bimolecular rate constant k_2 of $1.33 \times 10^{-1}\ \text{M}^{-1}\,\text{s}^{-1}$ for the dioxygen activation of the $Cu^{I}Cu^{I}Cu^{I}$ cluster. This second-order rate constant is similar to values that we have previously determined for the dioxygen activation of other model tricopper clusters at room temperature.[7,8]

The process can be made catalytic by adding the appropriate amounts of H_2O_2 to regenerate the spent catalyst after O-atom transfer from the activated tricopper complex to CH_4. This multiple-turnover reaction is depicted in Figure 1C. In these experiments, the $[Cu^{I}Cu^{I}Cu^{I}($**7-N-Etppz**$)]^{1+}$ catalyst is activated by O_2 as in the single-turnover experiment described earlier, but the spent catalyst is regenerated by two-electron reduction by a molecule of H_2O_2 (Figure 2A). Because the effective turnover number (TON), or the total equivalent of products formed over the time course of the experiment, peaks at approximately six when the turnover is initiated with 20 equivalents of H_2O_2, it is evident that abortive cycling begins to kick in when the steady-state concentration of the H_2O_2 concentration exceeds approximately ten equivalents. When the steady-state H_2O_2 concentration is above this level, reductive abortion of the activated catalyst becomes competitive with the O-atom transfer to methane to produce methanol. In this case, the rate of O-atom transfer is limited by the relatively low solubility of CH_4 in ACN under ambient conditions of temperature and pressure (Figure 2B).

The $[Cu^{I}Cu^{I}Cu^{I}($**7-N-Etppz**$)]^{1+}$ complex also mediates the catalytic oxidation of normal C2–C6 alkanes (data not shown)

---

[*] Prof. Dr. S. I. Chan, Y.-J. Lu, Dr. P. Nagababu, Dr. S. Maji, M.-C. Hung, P. D. Minh, J. C.-H. Lai, K. Y. Ng, Prof. Dr. S. S.-F. Yu
Institute of Chemistry, Academia Sinica
Nankang, Taipei 11529 (Taiwan)
E-mail: sunneychan@yahoo.com
sfyu@gate.sinica.edu.tw
M. M. Lee, S. Ramalingam, Prof. Dr. M. K. Chan
Department of Chemistry and Biochemistry, Ohio State University
Columbus, OH 43210 (USA)
E-mail: chan@chemistry.ohio-state.edu
Prof. Dr. I.-J. Hsu
Department of Molecular Science and Engineering
National Taipei University of Technology
Taipei 10608 (Taiwan)

[**] This work is supported by funds from Academia Sinica and Ohio State University (OSU), and grants from the National Science Council of the Republic of China (NSC 95-2113M-001-046, 97-2113M-001-027, and 98-2113M-001-026 to S.I.C.; 96-2627M-001-006 and 97-2113M-001-006-MY3 to S.S.F.Y.). S.R. was supported by a summer research fellowship from the National Science Foundation, USA (DBI 0750631). We acknowledge the assistance of Dr. Jyh-Fu Lee and his staff at the National Synchrotron Radiation Research Center, Hsinchu, Taiwan with the X-ray absorption measurements.

Supporting information for this article, including experimental details on the synthesis and characterization of the tricopper-peptide complexes, the biomimetic tricopper complexes, and the TEL-SAM protein and studies of the methane oxidation, is available on the WWW under http://dx.doi.org/10.1002/anie.201209846.

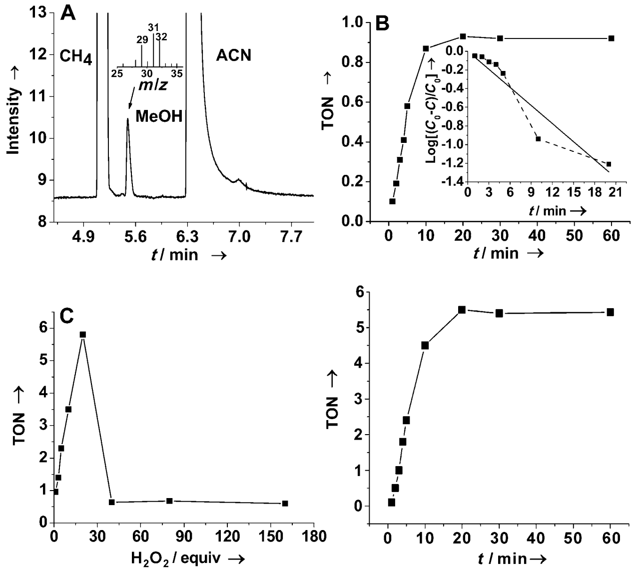

Figure 1. Methane oxidation by O_2, mediated by the tricopper $Cu^{I}Cu^{I}Cu^{I}$(**7-N-Etppz**)$^{1+}$ complex. A) Formation of methanol was analyzed by GC (retention time: 5.5 min); inset: assignment of the product peak to CH_3OH was verified by GC–MS, comparing the mass distribution with that of a CH_3OH standard. B) The time course of methane oxidation; inset: pseudo first-order kinetic plot with rate constant $k_1 = 0.0646\ \text{min}^{-1}$ (C_0 = initial concentration of the fully reduced tricopper complex; C = concentration of methanol produced at any given time), with the best straight-line fit to the data. C) Left: Catalytic turnover showing the TON as a function of the equivalents of H_2O_2 added to regenerate the spent catalyst; right: time course of catalytic methane hydroxylation by multiple turnovers of the tricopper complex in the presence of 20 equivalents of H_2O_2.

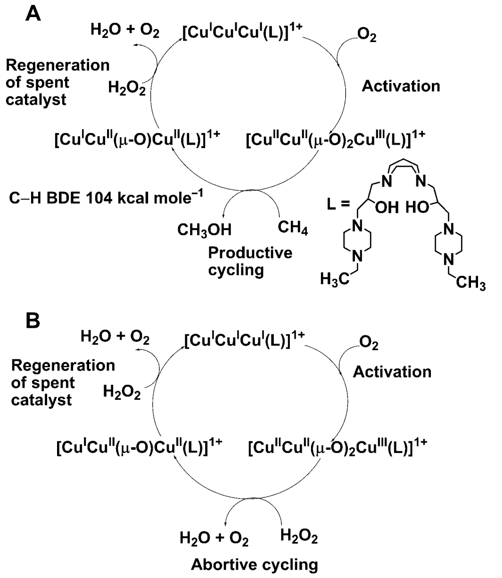

Figure 2. A) Productive cycling and B) abortive cycling in the oxidation of methane by O_2, mediated by the $Cu^{I}Cu^{I}Cu^{I}$(**7-N-Etppz**)$^{1+}$ complex in the presence of H_2O_2 as the sacrificial reductant. BDE = bond dissociation energy.

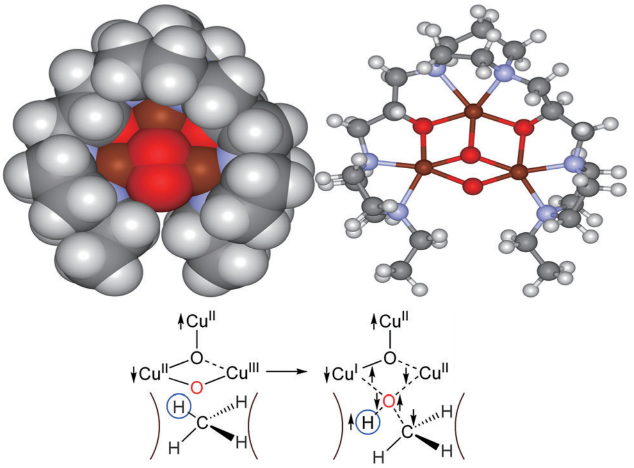

Figure 3. Space-filling model (left) and ball-and-stick model (right) of the optimized structure of $[Cu^{II}Cu^{II}(\mu\text{-}O)_2Cu^{III}$(**7-N-Etppz**)$]^{1+}$ showing the funnel-like opening or cleft at the bottom for a hydrocarbon substrate to access the "hot" oxene group. H white, C gray, N blue, O red, Cu brown. Formation of the transition-state complex during facile singlet oxene transfer to methane from a dioxygen-activated tricopper complex is shown at the bottom.

to their corresponding alcohols and ketones with high efficiencies at room temperature. In these studies, we have used H_2O_2 to activate the $Cu^{I}Cu^{I}Cu^{I}$ complex to its $[Cu^{II}Cu^{II}(\mu\text{-}O)_2Cu^{III}$(**7-N-Etppz**)$]^{1+}$ catalytic intermediate as well as to regenerate the spent catalyst for multiple turnovers, as we have previously done with other tricopper complexes in the oxidation of cyclohexane, benzene, and styrene.[4,5] The catalytic cycle becomes more economical if the tricopper catalyst is activated with H_2O_2 in lieu of O_2 when the substrate is sufficiently soluble in the solvent to favor O-atom transfer over competitive reductive abortion of the activated catalyst at the higher concentration of H_2O_2 used.[4] Space-filling and ball-and-stick models of the structure of $[Cu^{II}Cu^{II}(\mu\text{-}O)_2Cu^{III}$(**7-N-Etppz**)$]^{1+}$ intermediate optimized by the semi-empirical PM6 method are shown in Figure 3 together with a depiction of the singlet oxene transfer across one of the C−H bonds in methane.[3]

To underscore the significance of the above results with respect to the putative tricopper cluster in the pMMO enzyme,[9] we have prepared a tricopper peptide complex based on the HIHAMLTMGDWD fragment of PmoA that lines the empty hydrophilic cavity at the D site in the X-ray crystal structure of the pMMO purified from *Methylococcus capsulatus* (Bath)[10] and have shown that it is capable of mediating facile methane oxidation at room temperature as well. The HIHAMLTMGDWD peptide binds three copper ions to form $Cu^{I}Cu^{I}Cu^{I}$- and $Cu^{II}Cu^{II}Cu^{II}$-peptide complexes in the presence of excess acetate or chloride (but not nitrate or sulfate). Both complexes are insoluble in aqueous buffer. The $Cu^{II}Cu^{II}Cu^{II}$-peptide complex forms a blue precipitate, and the precipitate for the $Cu^{I}Cu^{I}Cu^{I}$-peptide complex is white. The copper contained in each peptide is 3.00 ± 0.05 Cu atoms for the $Cu^{II}Cu^{II}Cu^{II}$-peptide complex and 3.08 ± 0.09 Cu atoms for the $Cu^{I}Cu^{I}Cu^{I}$-peptide complex, as determined by inductively coupled plasma optical-emission spectrometry (ICP OES). Fast atom bombardment mass spectrometry (FAB-MS) of the $Cu^{I}Cu^{I}Cu^{I}$-peptide complex embedded in a 3-nitrobenzyl alcohol matrix (Figure 4 A) reveals a mass peak at m/z 1613.7 ($z=1$), consistent with a Cu_3-peptide species. The corresponding 2:1 and 1:1 copper-peptide fragments are observed at m/z 1549.8–1551.8 ($z=1$),

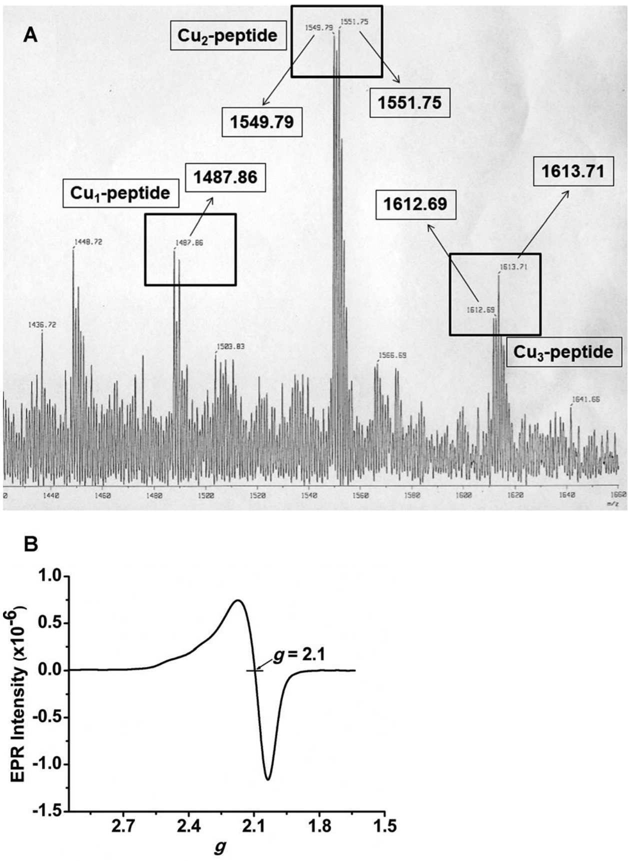

Figure 4. Characterization of the tricopper-peptide complex. A) FAB-MS of the solid $Cu^ICu^ICu^I$-peptide complex. The cluster of masses associated with the Cu_3-peptide complex hs been highlighted. B) 77 K EPR spectrum of the $Cu^{II}Cu^{II}Cu^{II}$-peptide complex. The blue precipitate was dispersed in KCl (1 % by weight) for EPR measurements.

and m/z 1487.9 ($z=1$), respectively. The $Cu^{II}Cu^{II}Cu^{II}$-peptide complex exhibits the featureless isotropic 77 K electron paramagnetic resonance (EPR) signal near $g \approx 2.1$, as previously reported for pMMO-enriched membranes and pMMO isolated from *Methylococcus capsulatus* (Bath),[3,11] providing a direct link between the tricopper-peptide complex and the putative tricopper cluster that has been implicated at the D site in the pMMO enzyme. This EPR signal has previously been simulated by a spin Hamiltonian for a triad of ferromagnetically coupled Cu^{II} spins in the $S_T = 3/2$ ground state ($J \approx 15$–$20\ cm^{-1}$) with an axial zero-field splitting $D = +0.017\ cm^{-1}$ and $E/D = 0.15$.[11]

Structural elucidation of the $Cu^{II}Cu^{II}Cu^{II}$-peptide complex is shown by the ligand structure deduced from K-edge extended X-ray absorption fine structure (EXAFS). To obtain high quality data, the peptide is covalently linked to the C-terminus of the TEL-SAM protein (see the Supporting Information). The EXAFS spectrum of the $Cu^{II}Cu^{II}Cu^{II}$-protein complex formed by treating the TEL-SAM-PmoA-(38–49) fusion protein with $Cu(OAc)_2$ is shown in Figure 5. The average first-shell (O/N), S, and Cu coordination numbers of the three copper ions are 3, 0.3, and 2, respectively, in excellent agreement with the ligand structure of the tricopper cluster modeled earlier into the D site of the enzyme.[9] The corresponding Cu–ligand distances and details on the fitting of the EXAFS data are provided as insets in Figure 5. The fitting requires a capping oxo group, to account for the ferromagnetic coupling among the three Cu^{II} ions inferred for the cluster from the EPR spectra (Supporting Information, Figure S5). The assignment of the observed EPR signal to the $S_T = 3/2$ ground state of a triad of ferromagnetically coupled Cu^{II} spins is confirmed by magnetic susceptibility measurements on the $Cu^{II}Cu^{II}Cu^{II}$-peptide complex (Supporting Information, Figure S6).

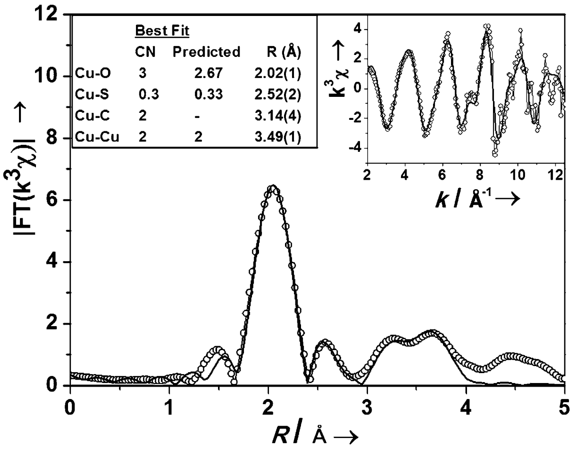

		O,N	S	Cu
Cu K-edge				
EXAFS	Cu1	3	0	2
Predictions	Cu2	2	1	2
	Cu3	3	0	2
Average		2.67	0.33	2

Figure 5. Cu K-edge EXAFS spectrum for the TEL-SAM-PmoA(38–49) fusion protein with the peptide sequence HIHAMLTMGDWDPD; left inset: best fit of the ligand structure for the tricopper cluster. Right inset: the fitted $k^3\chi(k)$ data. The average coordination numbers (CN) predicted from the ligand structure proposed in an earlier model of the D site[9] are shown below.

EXAFS data have also been collected for the $Cu^{II}Cu^{II}Cu^{II}$- and $Cu^ICu^ICu^I$-peptide complexes without the TEL-SAM protein, and these results are compared in Figure S8 and Table S2 of the Supporting Information. The measurements on the $Cu^ICu^ICu^I$-peptide complex were undertaken at 100 K to suppress artifacts arising from the extreme sensitivity of the complex to traces of dioxygen in the sample. Analysis of the EXAFS data indicates that the structure of the $Cu^ICu^ICu^I$ triad in the complex is similar to that of the oxidized cluster, but without the capping oxo group. The Cu–Cu distance has also increased to approximately 4 Å from 3.5 Å in the $Cu^{II}Cu^{II}Cu^{II}$-peptide complex, as expected.

The peptide **H**IHA**M**LTMG**D**W**D** provides the bulk of the potential metal-ligating residues of the PmoA fragment that we have previously used to build the tricopper cluster into the D site of the crystal structure of pMMO.[9] The residues highlighted in bold in the peptide sequence correspond (from left to right) to His38, Met42, Asp47, and Asp49 of PmoA and are found to be absolutely required for the formation of the tricopper-cluster complex, according to studies on peptide mutants with single amino-acid replacements (Supporting Information, Table S1). In the tricopper cluster modeled into the protein, the remaining ligands are provided by the carboxylate side-chains of Glu100 from PmoA and of Glu154 from PmoC. In the biomimetic tricopper-peptide complex, these carboxylates are replaced by exogenous anionic acetate or chloride in the peptide/copper solution during the formation of the tricopper-peptide complex.

Cu X-ray absorption near-edge spectroscopy (XANES) of the solid $Cu^{I}Cu^{I}Cu^{I}$-peptide complex confirms that the copper ions in the complex are fully reduced. XANES and EPR spectra reveal that the copper ions in the $Cu^{I}Cu^{I}Cu^{I}$-peptide complex are rapidly re-oxidized in the presence of air or dioxygen, as is observed for the putative tricopper cluster in pMMO (Supporting Information, Figure S8 A). However, upon activation of the $Cu^{I}Cu^{I}Cu^{I}$-peptide complex by dioxygen in the presence of propylene or methane, we observe rapid oxidation of these substrates. The dioxygen-activated tricopper-peptide complex is capable of mediating facile epoxidation of propylene, as well as methane oxidation. Because the $Cu^{I}Cu^{I}Cu^{I}$-peptide complex is insoluble in aqueous buffer, we have carried out oxidation of the substrate with the $Cu^{I}Cu^{I}Cu^{I}$-peptide complex encapsulated in mesoporous carbon (Figure 6). With propylene as the substrate, only propylene oxide is produced according to GC–MS. The maximum TON possible should then be one, assuming that all the tricopper-peptide complexes encapsulated in the mesoporous carbon are active, or can be activated by dioxygen. Based on the total product yield at the end of the two hour experiment, close to 80% of the $Cu^{I}Cu^{I}Cu^{I}$-peptide complexes have participated in the epoxidation of propylene (Figure 7 A). We can see from the time course of the reaction that the propylene epoxidation is extremely efficient. Over 50% of the expected propylene oxide is formed within ten minutes. The yield for methane oxidation is substantially lower, only 12% based on the tricopper-peptide complexes encapsulated in the mesoporus carbon over the two hour experiment (Figure 7 B). These experiments clearly demonstrate that the $Cu^{I}Cu^{I}Cu^{I}$-peptide complex is capable of mediating facile O-atom transfer to organic substrates upon activation by dioxygen.

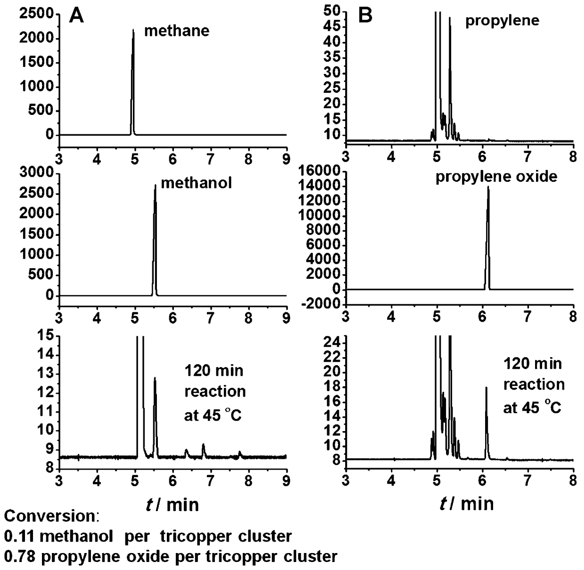

Figure 6. Gas chromatograms recorded for the oxidation of A) methane and B) propylene by O_2, mediated by the $Cu^{I}Cu^{I}Cu^{I}$-peptide complex. The reactants and products were identified by GC–MS.

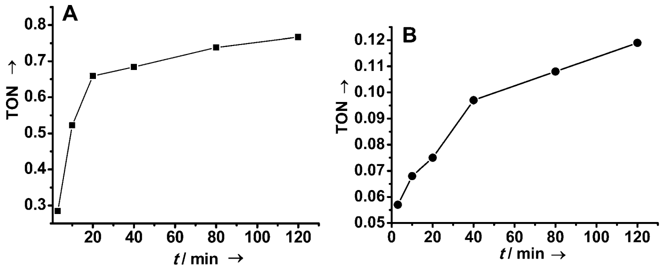

Figure 7. Time-course experiments showing A) the conversion of propylene into propylene oxide and B) the oxidation of methane into methanol by O_2, mediated by the $Cu^{I}Cu^{I}Cu^{I}$-peptide complex.

In summary, we have reported herein two tricopper complexes that are capable of facile conversion of methane to methanol: a tricopper-peptide complex derived from pMMO and a biomimetic model tricopper complex. Previously, a number of catalytic systems have also been developed for methane oxidation.[12–15] They all function at high temperatures and several are heterogeneous systems operating in zeolites.[16–18] Our biomimetic tricopper complex oxidizes methane efficiently at room temperature and can be formulated either as a homogeneous or heterogeneous catalyst. It is a functional catalyst based on the physicochemical principles acquired from understanding the structure and reactivity of the putative tricopper cluster in the copper monooxygenase.

Received: December 10, 2012

Keywords: biocatalysis · bioinorganic chemistry · catalysis · C-H activation · tricopper complex

---

[1] L. Que, W. B. Tolman, *Nature* **2008**, *455*, 333.
[2] S. Friedle, E. Reisner, S. J. Lippard, *Chem. Soc. Rev.* **2010**, *39*, 2768.
[3] S. I. Chan, S. S.-F. Yu, *Acc. Chem. Res.* **2008**, *41*, 969.
[4] S. I. Chan, C. Y.-C. Chien, C. S.-C. Yu, P. Nagababu, S. Maji, P. P.-Y. Chen, *J. Catal.* **2012**, *293*, 186.
[5] P. Nagababu, S. Maji, M. P. Kumar, P. P.-Y. Chen, S. S.-F. Yu, S. I. Chana, *Adv. Synth. Catal.* **2012**, *354*, 3275.

[6] D. T. Sawyer, A. Sobkowiak, J. L. Roberts, Jr., *Electrochemistry For Chemists*, Wiley, New York, 2nd ed., **1995**, p. 505.

[7] P. P.-Y. Chen, R. B.-G. Yang, J. C.-M. Lee, S. I. Chan, *Proc. Natl. Acad. Sci. USA* **2007**, *104*, 14570.

[8] S. Maji, J. C.-M. Lee, Y.-J. Lu, C.-L. Chen, M.-C. Hung, P. P.-Y. Chen, S. S.-F. Yu, S. I. Chan, *Chem. Eur. J.* **2012**, *18*, 3955.

[9] S. I. Chan, V. C.-C. Wang, J. C.-H. Lai, S. S.-F. Yu, P. P.-Y. Chen, K. H.-C. Chen, C.-L. Chen, M. K. Chan, *Angew. Chem.* **2007**, *119*, 2038; *Angew. Chem. Int. Ed.* **2007**, *46*, 1992.

[10] R. L. Lieberman, A. C. Rosenzweig, *Nature* **2005**, *434*, 177.

[11] K. H.-C. Chen, C.-L. Chen, C.-F. Tseng, S. S.-F. Yu, S.-C. Ke, J.-F. Lee, H. H.-T. Nguyen, S. J. Elliott, J. O. Alben, S. I. Chan, *J. Chin. Chem. Soc.* **2004**, *51*, 1081.

[12] R. A. Periana, D. J. Taube, S. Gamble, H. Taube, T. Satoh, H. Fujii, *Science* **1998**, *280*, 560.

[13] R. A. Periana, D. J. Taube, E. R. Evitt, D. G. Löffler, P. R. Wentrcek, G. Voss, T. Masuda, *Science* **1993**, *259*, 340.

[14] A. Tomita, J. Nakajima, T. Hibino, *Angew. Chem.* **2008**, *120*, 1484; *Angew. Chem. Int. Ed.* **2008**, *47*, 1462.

[15] N. Dietl, M. Schlangen, H. Schwarz, *Angew. Chem.* **2012**, *124*, 5638; *Angew. Chem. Int. Ed.* **2012**, *51*, 5544.

[16] M. H. Groothaert, P. J. Smeets, B. F. Sels, P. A. Jacobs, R. A. Schoonheydt, *J. Am. Chem. Soc.* **2005**, *127*, 1394.

[17] E. M. Alayon, M. Nachtegaal, M. Ranocchiari, J. A. van Bokhoven, *Chem. Commun.* **2012**, *48*, 404.

[18] C. Hammond, M. M. Forde, M. H. Ab Rahim, A. Thetford, Q. He, R. L. Jenkins, N. Dimitratos, J. A. Lopez-Sanchez, N. F. Dummer, D. M. Murphy, A. F. Carley, S. H. Taylor, D. J. Willock, E. E. Stangland, J. Kang, H. Hagen, C. J. Kiely, G. J. Hutchings, *Angew. Chem.* **2012**, *124*, 5219; *Angew. Chem. Int. Ed.* **2012**, *51*, 5129.